



Temperature dependence of surface composition and morphology in polymer blend film

Jichun You^a, Tongfei Shi^{a,*}, Yonggui Liao^a, Xinglin Li^b, Zhaohui Su^{a,*}, Lijia An^{a,*}

^aState Key Laboratory of Polymer Physics and Chemistry, Changchun Institute of Applied Chemistry, Chinese Academy of Sciences, Changchun 130022, China

^bNational Analytical Research Center of Electrochemistry and Spectroscopy, Changchun Institute of Applied Chemistry, Chinese Academy of Sciences, Changchun 130022, China

ARTICLE INFO

Article history:

Received 28 January 2008

Received in revised form 13 May 2008

Accepted 28 July 2008

Available online 3 August 2008

Keywords:

Polymer blend

Surface composition

In situ XPS

ABSTRACT

Thin films of poly(methyl methacrylate) (PMMA) and poly(styrene-*ran*-acrylonitrile) (SAN) blend can phase separate upon heating to above its critical temperature. Temperature dependence of the surface composition and morphology in the blend thin film upon thermal treatment was studied using *in situ* X-ray photoelectron spectroscopy (XPS) and *in situ* atomic force microscopy (AFM). It was found that in addition to phase separation, the blend component preferentially diffused to and aggregated at the surface of the blend film, leading to the variation of surface composition with temperature. At 185 °C, above the critical temperature, the amounts of PMMA and SAN phases were comparable. At lower temperatures PMMA migrated to the surface, leading to a much higher PMMA surface content than in the bulk. The migration and preferential segregation of a blend component in thin films demonstrated here are responsible for the great difference between *in situ* and *ex situ* experimental (not real quenching or annealing) results of polymer blend films, and help explain the slow kinetics of surface phase separation at early stage for blend thin films reported in literature. This is significant for the control of surface properties of polymer materials.

© 2008 Elsevier Ltd. All rights reserved.

1. Introduction

Polymer blend films play an important role in many applications, such as biomaterials, adhesion, electrochemistry, and surface patterning [1–3]. Their performance in these applications depends on surface properties, which are mainly controlled by surface composition and surface structures. On the other hand, surface properties of thin films can be different from that of the bulk because molecules at surface are exposed to a different environment [4]. Polymer blend thin films are no exceptions.

Much work has been focused on the relationship between surface composition and structure and surface properties of thin films [5–12]. In addition, by using techniques such as atomic force microscopy (AFM) [13,14], forward recoil spectrometry (FRS) [15], and dynamic secondary ion mass spectrometry (DSIMS) [16], morphology, composition distribution in the planes parallel and vertical to the substrate, and phase evolution and dynamics [13–20] have been studied. So far most of the investigations on the

evolution of surface chemical composition and surface structure have been based on *ex situ* experimental methods. Recently *in situ* AFM and XPS techniques have been employed to investigate the evolution of surface structure and surface composition in real time and direct space, such as crystallization and melting of polymers [21–23], island nucleation and growth in self-assembled monolayers [24], and substrate-facilitated assembly of elastin-like peptides [25]. In some cases, significant discrepancies in surface composition or surface structure have been found between *ex situ* and *in situ* experiments, such as in thin blend films of poly(methyl methacrylate) (PMMA) and poly(styrene-*ran*-acrylonitrile) (SAN). PMMA/SAN is a typical system for phase separation studies [13,15,19,26–31]. Based on the results obtained via *ex situ* experiments [13,15,19,26], the surface of the blend film is covered with PMMA-rich phase even after extensive annealing. However, more recently *in situ* AFM studies showed that at high temperatures surface phase separation is obvious, and both PMMA-rich phase and SAN-rich phase are present at the film surface [30]. The discrepancy observed suggests that the decrease of temperature after the annealing process can significantly alter the surface composition of the blends. In fact, many polymer materials are processed at high temperatures before cooled down to and used at low temperatures. If surface structure and surface composition are important to a particular application, the effect of the cooling

* Corresponding authors. Tel.: +86 431 85262137/+86 431 85262854; fax: +86 431 85262969.

E-mail addresses: tfshi@ciac.jl.cn (T. Shi), zhsu@ciac.jl.cn (Z. Su), ljan@ciac.jl.cn (L. An).

process on the surface composition and structure must be considered. However, so far the literature on the evolution of surface structure and surface composition with decreasing temperature is limited.

In this work, *in situ* XPS and AFM were employed to examine the evolution and development of the surface chemical composition and surface morphology of thin films of PMMA–SAN blends during various annealing processes. It was found that at higher temperatures, the amounts of PMMA and SAN on the surface were comparable. When temperature decreased, PMMA migrated to the surface and takes the place of SAN. Based on these observations, the difference between *in situ* and *ex situ* experimental results of polymer blend films reported by previous researchers was clarified, and the slow kinetics of surface phase separation at early stage in our previous work was explained.

2. Experiment part

2.1. Materials

Poly(methyl methacrylate) (PMMA, $M_w = 387$ kg/mol, PD = 3.72; Across) and poly(styrene-*ran*-acrylonitrile) (SAN, 30% AN by mass, $M_w = 149$ kg/mol, PD = 2.66; Aldrich) were used as received without any further purification.

2.2. Sample preparation

Thin films of a PMMA/SAN blend (50/50 wt%) were prepared by spin-casting a 1.0×10^{-2} g/mL solution of the blend in 1,2-dichloroethane onto silicon wafers. The silicon wafers were cleaned in a bath of 100 mL of 80% H₂SO₄, 35 mL of 30% H₂O₂, and 15 mL of deionized water at 80 °C for 60 min, rinsed with deionized water, and then dried with nitrogen [20] prior to use. Four replicate films were prepared under the above conditions and labeled as samples #1, #2, #3, and #4. The thicknesses of all films were measured on a Bruker D8 Discover X-ray reflectometer to be 130 ± 2.3 nm (this thickness is well-suited to compare with that in Ref. [30]).

2.3. Atomic force microscopy (AFM)

The surface phase morphology of the blend films was characterized on a Seiko SPA-300 scanning probe microscope equipped with a temperature-control stage operating in tapping mode. Sample #1 was treated in the chamber of the AFM according to the temperature profile shown in Fig. 1.

2.4. X-ray photoelectron spectroscopy (XPS)

Surface chemical composition of the films was determined on a Thermo ESCALAB 250 X-ray photoelectron spectrometer equipped with a hot stage using monochromatic Al X-ray source (1486.6 eV). The take-off angle (between the sample surface and the detector optics) was 90°. The sample analysis chamber of the XPS instrument was maintained at a pressure of about 2.0×10^{-7} Pa during the spectral measurements. The binding energy peaks were charge-referenced to the C–C/C–H peak at 284.6 eV [32]. The area exposed to X-ray was about $500 \times 500 \mu\text{m}^2$, and the sampling depth was less than 10 nm.

To assess the extent of degradation of the blend films caused by the X-ray at high temperatures, sample #2 was maintained at 185 °C for several hours in the XPS analysis chamber to reach a steady state, and spectra were taken at 0 min, 2 min, 4 min, 6 min, and 8 min of X-ray exposure, respectively, at the same sample position. In addition, sample #3 was heated to 185 °C in an oven for about 3 h, which approximately corresponds to point E in Fig. 1, and then quenched into liquid nitrogen. Sample #4 was treated using

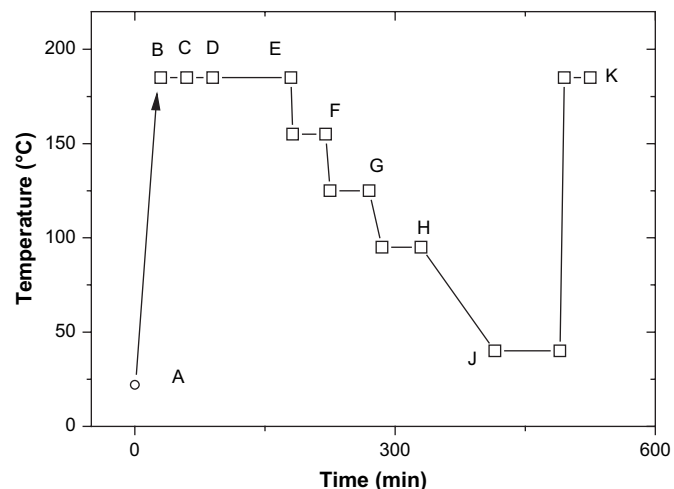


Fig. 1. Schematic representation of thermal treatment profile for samples #1 and #4. Measurements are carried out at the labeled point.

the temperature profile shown in Fig. 1, and the surface composition was monitored by XPS.

To assess the evolution of the surface chemical composition and morphology of the PMMA/SAN blend films, the following thermal treatment process shown in Fig. 1 was applied to samples #1 and #4, *in situ* on the AFM and XPS, respectively. First the specimen was rapidly heated to 185 °C (A and B), and then maintained at this temperature for about 3 h for the phase separation to fully develop (B–E). The specimen was then cooled to 155 °C, 125 °C, 95 °C, and 40 °C and maintained for 38 min, 45 min, 45 min, and 75 min, respectively (E–J), to simulate the slow cooling process used in *ex situ* experiments reported in literature. Finally the film was heated quickly back to 185 °C and maintained at the temperature for half an hour to investigate if the change of the surface morphology and composition was reversible (J–K).

3. Results and discussion

The binary mixture of PMMA/SAN shows Lower Critical Solution Temperature (LCST) behavior. The critical phase separation temperature of this system is about 165 °C in the bulk, which is lower than the 185 °C used in this work for the phase separation to develop. The glass transition temperature of PMMA and SAN is 119.5 °C and 112.0 °C, respectively (from DSC, data not shown).

3.1. Temperature dependence of surface phase separation

Fig. 2 shows the snapshots of topography (left) and phase (right) images of the film surface (sample #1) obtained at each stage of the thermal treatment according to Fig. 1. Before heated, the sample has the flat surface (Fig. 2A). When the sample is annealed at 185 °C for 30 min (Fig. 2B), the surface becomes uneven. From then on, the topography images show that the height increases with increasing time during annealing (Fig. 2C–E) and decreases with decreasing the annealing temperature (F–J). When the sample is heated to 185 °C again, its surface becomes uneven again (Fig. 2K). The phase images change with time in a different way. It is obvious that the film surface is homogeneous before the thermal treatment (Fig. 2a). Darker and lighter regions at the surface appear when the temperature reaches 185 °C (Fig. 2b), and these regions further develop with time at this temperature (c–e). As the temperature decreases from 185 °C to 95 °C, the process is reversed, and the surface becomes rather uniform at 50 °C (Fig. 2j). As the temperature increases back to 185 °C, the film surface becomes

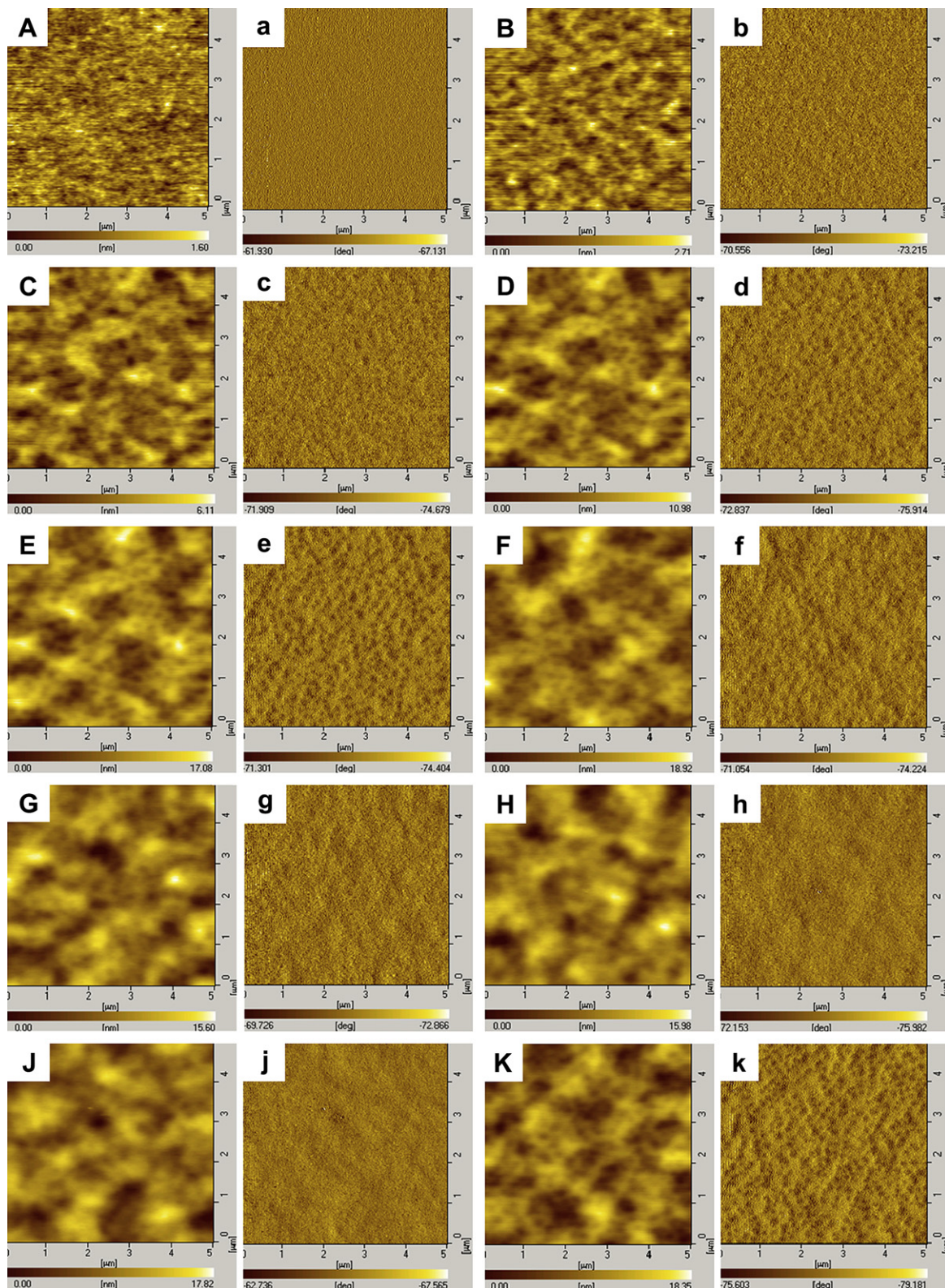


Fig. 2. Snapshots of topography and phase images ($5 \times 5 \mu\text{m}^2$) of sample #1 at various temperatures and time corresponding to Fig. 1.

inhomogeneous again (Fig. 2k). According to our previous study, in the phase images of PMMA/SAN blend thin films the darker regions are PMMA-rich phase, and the lighter regions are SAN-rich phase [30]. It is very interesting that there are some small “dark” regions on the uneven surface in the topography images, which appear as “darker” regions in the corresponding phase images, when the

phase separation has developed deeply [Fig. 2E(e) and K(k)]. Possible reason for this is the different thermal expansion coefficients and density of PMMA and SAN at this temperature. These observations confirm that for a 50/50 PMMA/SAN blend film, at higher temperatures the blend enters a two-phase region, and the surface becomes inhomogeneous and phase separates into

PMMA-rich and SAN-rich phases. When the temperature decreases, the film surface becomes homogeneous. Fig. 3 shows the development of the RMS (root-mean-square surface smoothness) obtained from the topography (RMS_h) and the phase (RMS_p) images during the above thermal treatment as shown in Fig. 1. It is obvious that both RMS_h and RMS_p reach a plateau after the initial slight increase. From then on, they have higher (Fig. 3J) and lower (F–I) magnitudes at 185 °C and lower temperature, respectively. There are two possible reasons for the evolution of the topography and phase images: the blend becomes miscible, or the PMMA- or the SAN-rich phase migrates to and covers the whole surface. According to previous *ex situ* experimental results by AFM and FReS [14,15], it is clear that this is still a phase separated system. Therefore in the temperature cycle, especially in the temperature decreasing process (Fig. 1E–J) the surface reconstruction may involve migration of one blend component from the bulk to the surface. To better understand this surface reconstruction process, XPS was utilized because it can assess the evolution of the surface composition quantitatively.

3.2. Degradation of PMMA

The thermal degradation temperature of PMMA and SAN is 234.2 °C and 373.2 °C, respectively, studied by thermogravimetric analysis (data not shown). Although the upper experimental temperature was about 50 °C below the degradation temperature of PMMA and much lower than that of SAN, blend film specimen may still be degraded due to the X-ray exposure in the XPS data acquisition, and this effect must be assessed before the quantitative analysis of the surface composition by the XPS technique. Fig. 4 shows the C1s region of the XPS spectra of sample #2 collected at different X-ray exposure time. Four bands in the spectra are clearly identified, which are assigned to the chemical groups found in PMMA and SAN molecules [33–35]. The band at 284.6 eV is assigned to the –CH₃ and –CH₂– species in PMMA or SAN, and the one at ~286.8 eV is due to the C–O moiety in the MMA units and the C≡N and CH entities in the α position to the nitrile group [34], while the peak at 288.8 eV is associated with the PMMA ester C (O–C=O) [33,34]. In addition there is an aromatic π – π^* shake-up peak at 291.3 eV. It can be seen that the peak for the ester C at 288.8 eV disappears very quickly, suggesting that the PMMA ester groups degrade more easily under X-ray exposure. To minimize the sample degradation in the data acquisition process, the acquisition time was reduced, and each measurement was done at a fresh position that had not been exposed to X-ray previously. In addition, the XPS

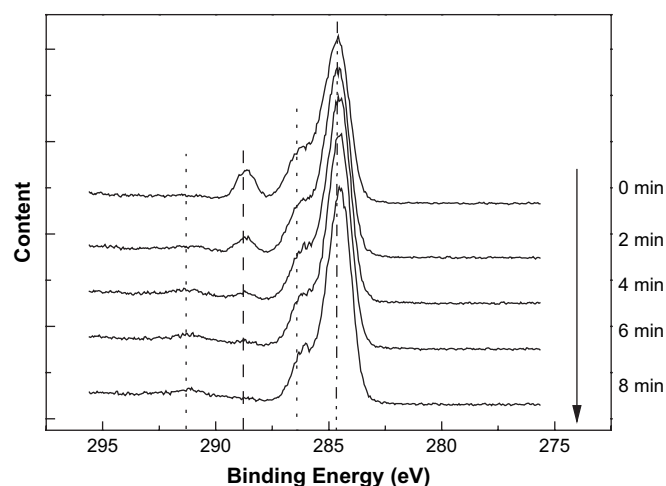


Fig. 4. C1s region of the XPS spectra of the blend thin film (sample #2) acquired at various X-ray exposure time at 185 °C [35].

composition for point E (see Fig. 1) obtained *in situ* under these conditions was compared with that of sample #3 (same thermal history as E) measured at room temperature, and they were within experimental error. These results indicate that even though degradation occurs in the blend film specimen, the procedure adopted in this study can effectively minimize the effect, and the XPS data thus obtained well represent the surface compositions quantitatively.

3.3. Temperature dependence of surface composition

Because there are two oxygen atoms in each MMA unit, and none in SAN units, the surface O/C atomic ratio calculated from the surface atomic concentrations measured by XPS is a good indication of the surface composition of PMMA/SAN blend films. Higher surface O/C ratio indicates higher PMMA content and lower SAN content at the surface. The evolution of the surface composition of the blend film was followed using the O/C ratio, and the result is plotted in Fig. 5. The upper and the lower dash lines represent the theoretical O/C ratios for pure PMMA and the PMMA/SAN (50/50) blend, respectively. It can be seen that the surface of the spin-coated blend film (point A) exhibits an O/C ratio higher than that of the bulk, but lower than that of pure PMMA. When the film is

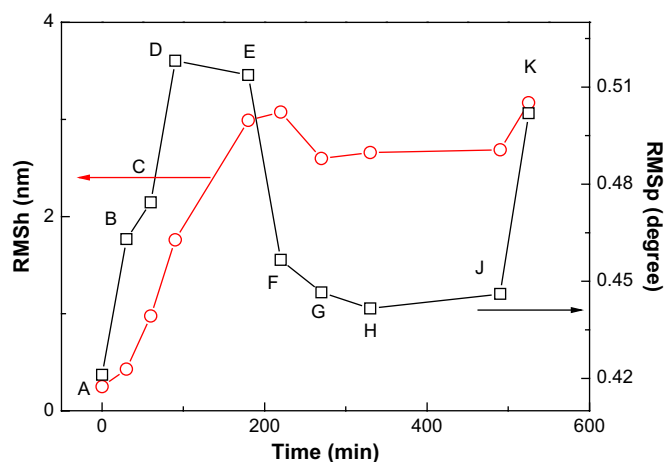


Fig. 3. Development of RMS_h and RMS_p during the thermal treatment corresponding to Fig. 1.

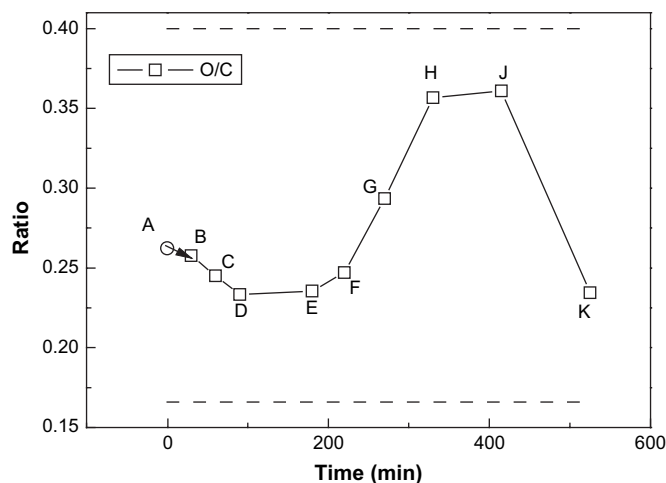


Fig. 5. Development of the XPS C1s peaks of sample #4 in the thermal treatment process described in Fig. 1.

quickly heated to 185 °C, the oxygen content starts to decrease (point B), and after annealing at this temperature (B–D) the surface composition reaches a steady state (D and E). When the temperature decreases, the oxygen content at the surface increases significantly (E–J), and at room temperature the surface oxygen content approaches that of pure PMMA. From XPS analysis it is obvious that at 185 °C (points D–F in Fig. 5) the surface O/C ratio is ~ 0.24 , which is close to that in the bulk of the blend (50/50 wt%). This indicates that significant amounts of both PMMA and SAN are at the surface. The above observations indicate that the surface of the as-cast film was covered with both PMMA and SAN, with PMMA in excess; increasing the temperature caused SAN to migrate to the surface, and at 185 °C it took ~ 90 min for the surface to reach a steady state, which consisted of comparable amount of PMMA and SAN; when the temperature decreased, PMMA moves to the surface, and eventually at room temperature, the surface was mostly PMMA. This assessment is also supported by the high resolution XPS spectra in the C1s region obtained, which are shown in Fig. 6.

For PMMA/SAN blend films prepared by spin-coating, there is a surface excess of PMMA due to higher solubility of PMMA in the solvent (1,2-dichloroethane) estimated by solubility parameters, i.e. in the spin-coating process, SAN is more quickly depleted from the solution and solidifies first onto the substrate [36], while PMMA tends to stay longer in the solution phase and enrich at the surface as more solvent is evaporated. Finally PMMA and SAN chains are frozen into a narrow zone before reaching a thermodynamically stable state since the solvent evaporates relatively fast in the spin-coating process. Upon heating to above the critical temperature of the blend, phase separation occurs in order to minimize the free energy of the system. At 185 °C, phase separation is obvious as shown by AFM (Fig. 2b–e and k), which is in good agreement with the *in situ* experiment results [37]. The weight fractions of the two phases are comparable, which is supported by XPS result according to above discussion. When the temperature decreases to below 185 °C but still above T_g (e.g. points F and G), the surface becomes more and more homogeneous, and the surface O/C atomic ratio becomes higher, which indicates that PMMA is migrating to the surface to partially displace SAN. In fact, in this whole process, several factors are important for the enrichment of a blend component and the phase separation at the film surface, including sample preparation history [38], interfacial tension [39], complex phase behavior [40], and the difference in the surface tension of the two components, which dominate the preferential surface segregation of one component in most cases. The complex migration

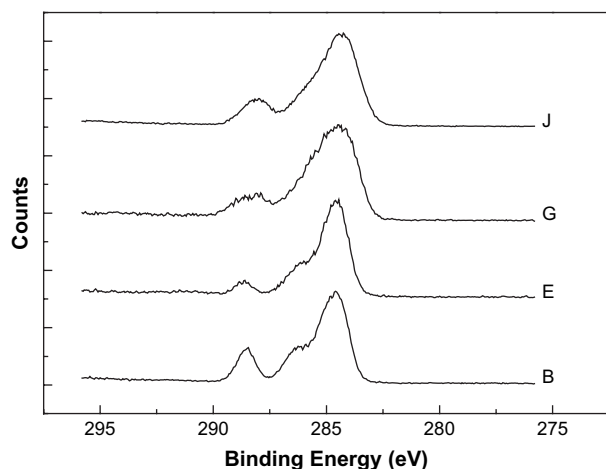


Fig. 6. Evolution of the surface composition of sample #4 represented by XPS O/C atomic ratio with the thermal treatment shown in Fig. 1. The upper and lower dash lines represent the theoretical O/C values in pure PMMA and the PMMA/SAN (50/50) blend, respectively.

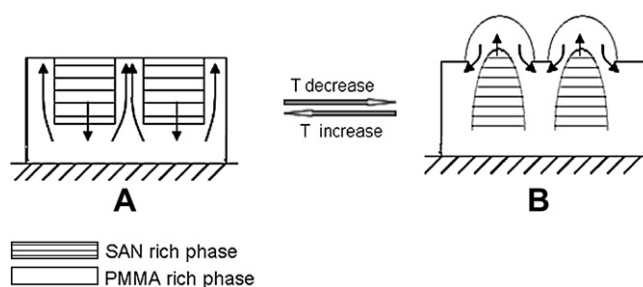


Fig. 7. Schematic representation of the surface phase migration between higher and lower temperatures.

may be caused by the difference in temperature dependence of surface tension and interfacial tension of PMMA and SAN. When the temperature is below T_g , the polymer chains are frozen, resulting in the stabilization of the morphology and the surface composition as observed by AFM and XPS at points H and J.

From point B to point E, it is a typical surface phase separation process, which we have previously reported [30]. In that work, PMMA/SAN blend films with the same thickness as used here was investigated by *in situ* AFM. The temporal evolution pattern of surface phase separation, especially the coalescence and merger process has been observed directly. The kinetics of this phase separation was discussed in detail. It was found that the function of the characteristic wave number and the annealing time exhibited two distinct regimes. The power exponent was about 0.12 in the first regime and 0.32 in the second regime, and the crossover point of the two regimes was at ~ 82 min, suggesting that the former stage is slower than the latter. Because no direct experimental evidence was available at that time, two possible reasons were speculated for the slow down of the surface phase separation kinetics observed. One was the diffusion of one component from the interior to the surface of the film, and the other was the restriction of polymer chain mobility by the 2D geometry constraint of the surface. The *in situ* XPS results obtained in the current work now provide direct evidence that the slower dynamics previously observed was due to the diffusion of the SAN component to the surface displacing PMMA. Further more, this diffusion reached equilibrium at about 90 min (as indicated by the steady O/C ratio from points D–E in Fig. 5), which is in good agreement with the *in situ* AFM result.

Based on the above discussion, the evolution of the surface composition can be interpreted as follows, as illustrated in Fig. 7: at 185 °C, due to the adjacent surface tension values of both components, there is comparable amount of both PMMA-rich phase and SAN-rich phase at the surface. When the sample is cooled from 185 °C to room temperature, PMMA migrates from the bulk to the surface of the film, while the system remains phase separated. The opposite process from B to A in Fig. 7 takes place when the sample is heated from room temperature to 185 °C. The evolution of the surface structure between these two states is reversible based on the *in situ* AFM [37] and XPS experiments, and the temperature dependence of the surface composition may be attributed to the change of the surface tension of the components with temperature.

4. Conclusion

We have investigated the evolution of the surface morphology and surface chemical composition of PMMA/SAN blend films using *in situ* XPS in addition to AFM, and found that when the film is heated to above the critical temperature, in addition to the phase separation of the two components, SAN also migrates to the surface. The migration of SAN to the surface at the early stage of phase separation can lead to the slower kinetics of surface phase

separation, which confirms our speculation in the previous report [30]. When the film is cooled down by annealing, PMMA preferentially aggregates at the surface to displace SAN. The entire process is reversible. These findings indicate that thermal treatment can strongly influence the surface composition and structure of blend thin films, which may be helpful to control surface properties of polymer films with multiple components.

Acknowledgement

This work is supported by the National Natural Science Foundation of China (50503022, 20423003) and the NSFC Fund for Creative Research Groups (50621302), and subsidized by the Special Funds for National Basic Research Program of China (2003CB615600).

References

- [1] Castro FA, Graeff CFO, Heier J, Hany R. *Polymer* 2007;48:2380.
- [2] Shi D, Hu GH, Ke Z, Li RKY, Yin JH. *Polymer* 2006;47:4659.
- [3] Liu K, Kiran E. *Polymer* 2008;49:1555.
- [4] Kajiyama T, Tanaka K, Ohki I, Ge SR, Yoon JS, Takahara A. *Macromolecules* 1994;27:7932.
- [5] Galicia P, Batina N, Gonzalez I. *J Phys Chem B* 2006;110:14398.
- [6] Ramana CV, Smith RJ, Hussain OM, Chusuei CC, Julien CM. *Chem Mater* 2005;17:1213.
- [7] Cioffi N, Losito I, Torsi L, Farella I, Valentini A, Sabbatini L, et al. *Chem Mater* 2002;14:804.
- [8] Hrapovic S, Luan BL, D'Amours M, Vatankhah G, Jerkiewicz G. *Langmuir* 2001;17:3051.
- [9] Gofer Y, Turgeman R, Cohen H, Aurbach D. *Langmuir* 2003;19:2344.
- [10] Zeng XQ, Moon S, Bruckenstein S. *Anal Chem* 1998;70:2613.
- [11] Chen Z, Ward R, Tian Y, Eppler AS, Shen YR, Somorjai GA. *J Phys Chem B* 1999;103:2935.
- [12] Indovina V, Occhiuzzi M, Pietrogiacomini D, Tuti S. *J Phys Chem B* 1999;103:9967.
- [13] Chung H, Wang H, Composto RJ. *Macromolecules* 2006;39:153.
- [14] Chung H, Ohno K, Fukuda T, Composto RJ. *Macromolecules* 2007;40:384.
- [15] Wang H, Composto RJ. *Interface Sci* 2003;11:237.
- [16] Slep D, Asselta J, Rafailovich MH, Sokolov J, Winesett DA, Smith AP, et al. *Langmuir* 1998;14:4860.
- [17] Sung L, Karim A, Douglas JF, Han CC. *Phys Rev Lett* 1996;76:4368.
- [18] Matsumoto M, Tanaka K, Azumi R, Kondo Y, Yoshino N. *Langmuir* 2004;20:8728.
- [19] Newby BZ, Composto RJ. *Phys Rev Lett* 2001;87:098302.
- [20] Wen GY, Li X, Liao YG, An LJ. *Polymer* 2003;44:4035.
- [21] Schönherr H, Frank CW. *Macromolecules* 2003;36:1199.
- [22] Schönherr H, Waymouth RM, Frank CW. *Macromolecules* 2003;36:2412.
- [23] Basire C, Ivanov DA. *Phys Rev Lett* 2000;85:5587.
- [24] Doudevski I, Schwartz DK. *J Am Chem Soc* 2001;123:6867.
- [25] Yang G, Woodhouse KA, Yip CM. *J Am Chem Soc* 2002;124:10648.
- [26] Lavoie A, Riedl B, Bousmina M. *J Polym Eng* 2007;27:129.
- [27] Bousmina M, Lavoie A, Riedl B. *Macromolecules* 2002;35:6274.
- [28] Hong ZY, Shaw MT, Weiss RA. *Macromolecules* 1998;31:6211.
- [29] Zheng Q, Peng M, Song YH, Zhao TJ. *Macromolecules* 2001;34:8483.
- [30] Liao YG, Su ZH, Ye XG, Li YQ, You JC, Shi TF, et al. *Macromolecules* 2005;38:211.
- [31] Kumaraswamy GN, Ranganathaiah C, Deepa Urs MV, Ravikumar HB. *Eur Polym J* 2006;42:2655.
- [32] Ton-That C, Shard AG, Daley R, Bradley RH. *Macromolecules* 2000;33:8453.
- [33] Ton-That C, Shard AG, Teare DOH, Bradley RH. *Polymer* 2000;42:1121.
- [34] Oultache AK, Prud'homme RE. *Polym Adv Technol* 2000;11:316.
- [35] (a) Jönsson SKM, Birgerson J, Crispin X, Greczynski G, Osikowicz W, Denier van der Gon AW, et al. *Synth Met* 2003;139:1;
(b) You JC, Li XL, Shi TF, Su ZH, An LJ. *Chem J Chin Univ* 2008;29:1495.
- [36] Li YX, Yang YM, Yu FS, Dong LS. *J Polym Sci Part B Polym Phys* 2006;44:9.
- [37] Liao YG, You JC, Li X, Sun ZY, Shi TF, An LJ. *Chem J Chin Univ* 2005;26:1777.
- [38] Lee WK, Tanaka K, Takahara A, Kajiyama T, Ha CS. *Bull Korean Chem Soc* 1997;18:958.
- [39] Mayes AM, Kumar SK. *MRS Bull* 1997;22:43.
- [40] Ogawa H, Kanaya T, Nishida K, Matsuba G. *Polymer* 2008;49:254.